CHIMERA STATES IN NETWORKS WITH HIERARCHICAL CONNECTIVITIES

Iryna Omelchenko
Institute of Theoretical Physics
Technische Universität Berlin
Germany
omelchenko@itp.tu-berlin.de

Stefan Ulonska
Institute of Theoretical Physics
Technische Universität Berlin
Germany
stefan.ulonska@fu-berlin.de

Alexander zur Bonsen
Institute of Theoretical Physics
Technische Universität Berlin
Germany
alexander@zurbonsen.de

Anna Zakharova
Institute of Theoretical Physics
Technische Universität Berlin
Germany
anna.zakharova@tu-berlin.de

Eckehard Schöll
Institute of Theoretical Physics
Technische Universität Berlin
Germany
schoell@physik.tu-berlin.de

Abstract

Chimera states are complex patterns that exhibit a hybrid structure combining coexisting spatial domains of coherent (synchronized) and incoherent (desynchronized) dynamics. Recent studies have demonstrated the appearance of chimera states in a variety of network topologies and for different types of individual dynamics. We analyse the emergence of chimera states in networks with complex coupling topologies arising in neuroscience and having hierarchical (quasi-fractal) connectivities. Two cases of individual node dynamics are considered: time-continuous Van der Pol oscillators, and time-discrete logistic maps. We elaborate the variety of chimera patterns in networks of different hierarchical levels, and study the role of network symmetries and clustering.

Key words

Synchronization, Networks, Chimera states, Van der Pol oscillators, Logistic maps

1 Introduction

Chimera states are peculiar type of dynamics when complex network exhibits a hybrid state combining both coherent and incoherent parts. The surprising aspect of this phenomenon is that these states were initially detected in systems of identical oscillators coupled in a symmetric ring topology with a symmetric interaction function and coexist with a completely synchronized state [Kuramoto and Battogtokh, 2002; Abrams and Strogatz, 2004]. The past decade has seen an increasing interest in chimera states [Panaggio and Abrams, 2015; Schöll, 2016], it was shown that they are not limited to phase oscillators but can be found in a large variety of different systems, including time-discrete maps, time-continuous chaotic models, neural systems, chemical oscillators, and optical systems. Different types of network topologies, including higher spatial dimensions, have been shown to support chimera-like patterns. Potential applications of chimera states in nature include the phenomenon of unihemispheric sleep, bump states in neural systems, power grids, social systems.

The motivation for studying irregular network topologies comes from recent results in the area of neuroscience. Diffusion tensor magnetic resonance imaging (DT-MRI) studies revealed an intricate architecture in the neuron interconnectivity of the human and mammalian brain. The analysis of DT-MRI images has shown that the connectivity of the neuron axons network represents a hierarchical geometry with fractal dimensions varying between 2.3 and 2.8, depending on the local properties, on the subject, and on the noise reduction threshold [Katsaloulis et al., 2009; Expert et al., 2011; Provata et al., 2012]. Based on these findings, we study the development of chimera states in networks which involve topologies with hierarchical connectivities. We uncover the influence of the irregular connectivity on the appearance and properties of chimera states.

2 An algorithm for construction of hierarchical connectivities

Topologies with hierarchical connectivities can be generated using a classical Cantor construction algorithm for a fractal set. This iterative hierarchical procedure starts from a *base pattern* or initiation string b_{init} of length b, where each element represents either a link

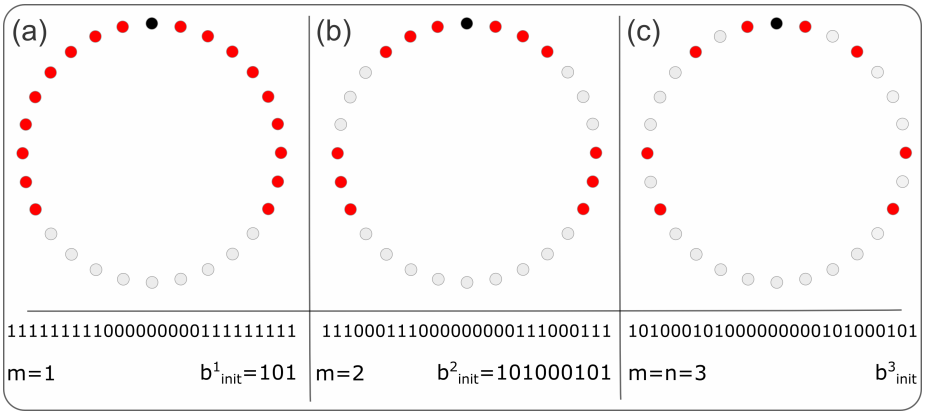

Figure 1. Transition from nonlocal to hierarchical connectivity via hierarchical steps m. The reference node is coloured in black, linked nodes in red and unconnected nodes (gaps) in grey. The initial base pattern of all panels is $b_{init} = (101)$, the level of hierarchy is $n = 3$, $N = b^n + 1 = 28$ nodes. (a) $m = 1$, each element in the initial base pattern is expanded by $\frac{27}{3} = 9$ elements and the final 1-step hierarchical system corresponds to nonlocal coupling where each element is coupled to its $R = 9$ nearest neighbours in both directions; (b) $m = 2$, expansion by $\frac{27}{9} = 3$ elements to a 2-step hierarchical system; (c) $m = n = 3$, fully hierarchical or $n-$step hierarchical system without further expansion of the base pattern.

('1') or a gap ('0'). The number of links contained in b_{init} is referred to as c_1. In each iterative step, each link is replaced by the initial base pattern, while each gap is replaced by b gaps. Thus, each iteration increases the size of the final bit pattern, such that after n iterations the total length is $N = b^n$. Since the hierarchy is truncated at a finite n, we call the resulting pattern hierarchical rather than fractal. Using the resulting string as the first row of the adjacency matrix $\mathbf{G}$, and constructing a circulant adjacency matrix $\mathbf{G}$ by applying this string to each element of the ring, a ring network of $N = b^n$ nodes with hierarchical connectivity is generated. We slightly modify this procedure by adding an additional zero in the first instance of the sequence, which corresponds to the self-coupling. This ensures the preservation of an initial symmetry of b_{init} in the final link pattern, which is crucial for the observation of chimera states. Thus a ring network of $N = b^n + 1$ nodes is generated. First, b_{init} is iterated m times according to the Cantor construction process, generating a pattern of size b^m. Afterwards, this pattern is expanded to the final size N by replacing each element with $\frac{N-1}{b^m}$ copies of itself.

Figure 1 demonstrates the simplest example of hierarchical connectivity for the initial base pattern $b_{init} = (101)$ and system size of $N = 27 + 1$ ($b = 3, n = 3$). In the following, an $m-$step hierarchical topology is denoted as $(b_{init})^m$, where b_{init} is the underlying base pattern, n the level of hierarchy and m the hierarchical step in a transition topology.

3 Networks of Van der Pol oscillators with hierarchical connectivities

We consider a ring of N identical Van der Pol oscillators with different coupling topologies, which are given by the respective adjacency matrix $\mathbf{G}$. While keeping the periodicity of the ring, and the circulant structure of the adjacency matrix, we vary the connectivity pattern of each element. The dynamical equations for the 2-dimensional phase space variable $\mathbf{x}_k = (u_k, \dot{u}_k)^T = (u_k, v_k)^T \in \mathbb{R}^2$ are:

$$\dot{\mathbf{x}}_i(t) = \mathbf{F}(\mathbf{x}_i(t)) + \frac{\sigma}{g} \sum_{j=1}^{N} G_{ij} \mathbf{H}(\mathbf{x}_j - \mathbf{x}_i) \quad (1)$$

with $i \in \{1, ..., N\}$. The dynamics of each individual oscillator is governed by

$$\mathbf{F}(\mathbf{x}) = \begin{pmatrix} v \\ \varepsilon(1 - u^2)v - u \end{pmatrix}, \quad (2)$$

where ε denotes the bifurcation parameter. The uncoupled Van der Pol oscillator has a stable fixed point at $\mathbf{x} = 0$ for $\varepsilon < 0$ and undergoes an Andronov-Hopf bifurcation at $\varepsilon = 0$. Here, only $\varepsilon > 0$ is considered. The parameter σ denotes the coupling strength, and $g = \sum_{j=1}^{N} G_{ij}$ is the number of links for each node (corresponding to the row sum of $\mathbf{G}$). The interaction is realized as diffusive coupling with coupling matrix $\mathbf{H} = \begin{bmatrix} 0 & 0 \\ b_1 & b_2 \end{bmatrix}$ and real interaction parameters b_1 and b_2, which are fixed as $b_1 = 1.0$ and $b_2 = 0.1$.

Besides the bifurcation parameter ε and the coupling strength σ, the topological quantities b_{init}, c_1, n, the resulting link density $\rho = \frac{c_1^n}{N}$ (for $m = n$) or $\rho = \frac{c_1^m b^{(n-m)}}{N}$ (for $m \neq n$) and fractal dimension $d_f = \ln c_1 / \ln b$ are important parameters in the study of networks with hierarchical connectivities. However, since there are several distributions of links for a given set of b and c_1 that result in unique topological structures, the arrangement of links in b_{init} has to be accounted

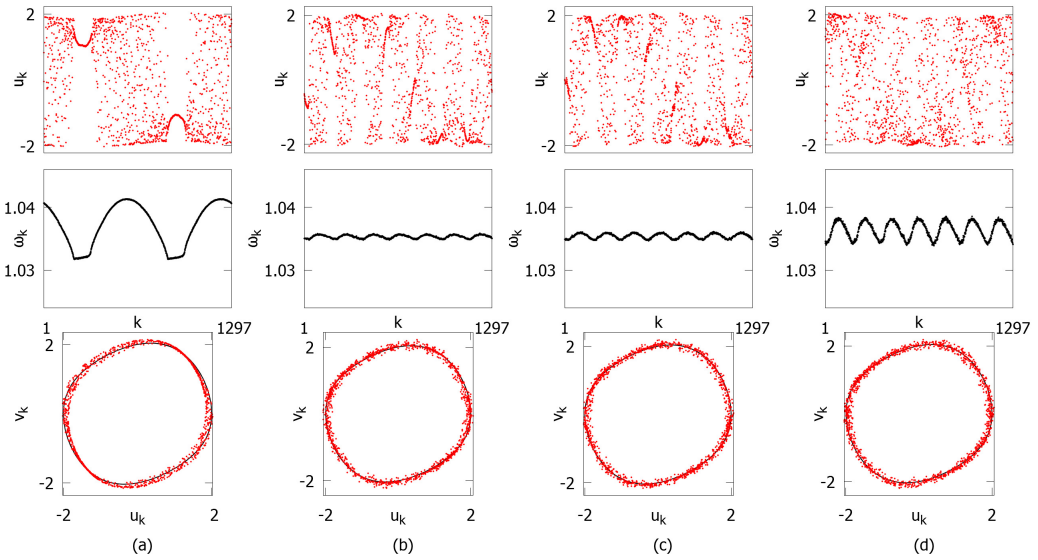

Figure 2. Chimera states in transiting topologies with $b_{init} = (110011)$, $n = 4$, $N = 1297$, $\sigma = 0.09$, $\varepsilon = 0.2$, random initial conditions. Snapshots of variables u_k (upper panels), mean phase velocities ω_k (middle panels), and snapshots in the phase space (u_k, v_k) (bottom panels, limit cycle of the uncoupled element shown in black). (a) $m = 1$, corresponding to nonlocal coupling with $r = 0.333$, clustering coefficient $C(110011, 4, 1) = 0.749142$, link density $\rho = 0.667$, $2-$chimera state; (b) $m = 2$, clustering coefficient $C(110011, 4, 2) = 0.559569$, link density $\rho = 0.444$, $7-$chimera; (c) $m = 3$, clustering coefficient $C(110011, 4, 3) = 0.414161$, link density $\rho = 0.298$, $7-$ chimera remains; (d) $m = n = 4$, fully hierarchical network with $7-$chimera and more pronounced ω_k profile, $C(110011, 4, 4) = 0.297791$ and $\rho = 0.197$.

for. Therefore, we consider the local clustering coefficient [Watts and Strogatz, 1998], which, for a network containing a set of nodes V and edges E, describes the number of links in the neighbourhood $N_i = \{v_j : e_{ij} \in E \vee e_{ji} \in E\}$ relative to the maximum number of links possible. If k_i is the number of neighbours for a node v_i, then maximum number of links is given by $k_i \cdot (k_i - 1)$ and the clustering coefficient C_i for a node v_i is defined as $C_i = \frac{|\{e_{jk} : v_j, v_k \in N_i, e_{jk} \in E\}|}{k_i(k_i-1)}$.

Figure 2 depicts an example of stepwise transition from nonlocal to hierarchical coupling for the symmetric base pattern (110011) with $n = 4$. For $m = 1$ we observe chimera state with two coherent domains, for further hierarchical steps the multiplicity of coherent domains increases. Similar properties show chimera states in the nonlocally coupled networks, there decreasing of the coupling range (number of links) causes increasing of the number of coherent domains for chimera states [Omelchenko, Provata et al., 2015; Omelchenko, Zakharova et al., 2015]. In regular topologies, chimera states often have even number of coherent domains, which appear in anti-phase, our observations show that more complex hierarchical topologies can generate chimera states with odd number of coherent domains as well.

We have provided extensive numerical simulations for a variety of hierarchical topologies, starting with different base patterns, and determined stability regimes in the plane of coupling strength and nonlinearity parameter of the individual oscillator, which show that chimera states indeed appear on the transition scenario between complete coherence and incoherence. The analysis of an exemplary network with larger base pattern, resulting in larger clustering coefficient and more complex network structure, has revealed two different types of chimera states highlighting the increasing role of amplitude dynamics.

Our analysis has identified the clustering coefficient and symmetry properties of the base pattern as crucial factors in classifying different topologies with respect to the occurrence of chimera states. Symmetric topologies with large clustering coefficients promote the emergence of chimera states, while they are suppressed by slight topological asymmetries or small clustering coefficients [Ulonska et al., 2016].

4 Networks of logistic maps with hierarchical connectivities

In previous work we have studied the transition from coherence to incoherence via chimera states in time-discrete ring networks of logistic maps with nonlocal coupling [Omelchenko et al., 2011]. This scenario has been explained analytically [Omelchenko et al., 2012], and realized experimentally [Hagerstrom et al., 2012].

In the current study, we analyse the influence of complex topologies with hierarchical connectivities on chimera patterns in networks of logistic maps. The sys-

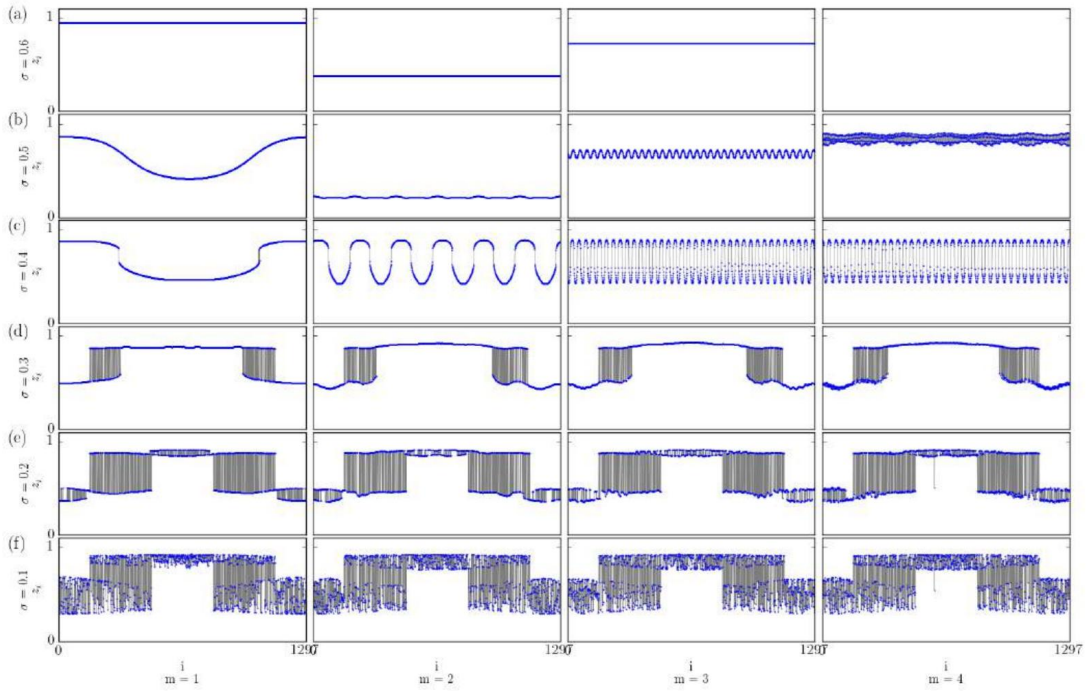

Figure 3. Snapshots for a network of $N = 1297$ logistic maps with base pattern $b_{init} = (110011)$. Columns correspond to hierarchical steps $m = 1, 2, 3, 4$, and the coupling strength $\sigma = 0.1, 0.2, 0.3, 0.4, 0.5, 0.6$ increases from bottom to top. Nonlinearity parameter of individual logistic map $a = 3.8$.

tem under consideration is a ring of N logistic maps:

$$z_i^{t+1} = f(z_i^t) + \frac{\sigma}{c_{n,m}} \sum_{j=0}^{N-1} C_{ij} \left[f(z_j^t) - f(z_i^t) \right], \quad (3)$$

where $f(z^t) = az^t(1-z^t)$, the coupling strength is denoted by σ, and $c_{n,m}$ refers to the number of links for the corresponding network node. The coupling matrix $\mathbf{C} = (C_{ij})$ describes hierarchical connectivity for chosen base pattern and hierarchical step, as described in previous sections. t denotes the discrete time, and a is a bifurcation parameter of the individual logistic map. We choose $a = 3.8$, thus the uncoupled map performs chaotic behaviour.

Selected mirror-symmetric base patterns, such as $b_{init} = (101)$, $b_{init} = (11011)$, $b_{init} = (110011)$, reproduce the nonlocal coupling topology at the initial hierarchical step $m = 1$. We uncover the evolution of chimera patterns on the transition to the higher hierarchical steps. Figure 3 depicts snapshots (at fixed time) for networks of $N = 1297$ maps with base pattern $b_{init} = (110011)$. Each column corresponds to a hierarchical step m, and the coupling strength σ decreases from top to bottom. In fact, higher hierarchical steps correspond to a diluted network with larger number of connectivity gaps, however, this does not destroy chimera patterns (panel d).

We have systematically investigated a variety of networks with different base patterns, and our findings show that symmetric patterns maintain chimera states, in agreement with our findings for time-continuous systems. The role of the coupling term in Eq. (3) has been elaborated, and different types of chimera states, as well as scenarios of their formation, have been investigated. We find stability regions for chimera states in the (σ, m) parameter plane, which show that chimera states can be observed at the transition from coherence to incoherence.

5 Conclusion

The properties of complex spatio-temporal patterns, named chimera states, in networks with hierarchical connectivities have been investigated. Considering two examples of time-continuous and time-discrete individual dynamics, we demonstrate a large variety of chimera patterns in networks with hierarchical connectivity. We uncover the role of topological properties, such as base patterns and symmetries, and demonstrate that additional complexity in the topologies can induce special types of chimera patterns, for instance nested chimeras, which are not possible to observe in regular nonlocal networks.

Acknowledgements

This work was supported by Deutsche Forschungsgemeinschaft in the framework of Collaborative Research Center SFB 910.

References

Kuramoto Y. and Battogtokh D. (2002) *Nonlinear Phenom. Complex Syst.*, **5**, 380.

Abrams D. M. and Strogatz S. H. (2004) *Phys. Rev. Lett.*, **93**, 174102.

Panaggio M. J. and Abrams D. M. (2015) *Nonlinearity* **28**, R67.

Schöll E. (2016) *Eur. Phys. J. Spec. Top.* **225**, 891.

Katsaloulis P., Verganelakis D. A., and Provata A. (2009) *Fractals* **17**, 181.

Expert P., Evans T. S., Blondel V. D., and Lambiotte R. (2011) *Proc. Natl. Acad. Sci. USA* **108**, 7663.

Provata A., Katsaloulis P., and Verganelakis D. A. (2012) *Chaos Soliton. Fract.* **45**, 174.

Watts D. J. and Strogatz S. H. (1998) *Nature* **393**, 440.

Omelchenko I., Provata A., Hizanidis J., Schöll E., Hövel P. (2015) *Phys. Rev. E* **91**, 022917.

Omelchenko I., Zakharova A., Hövel P., Siebert J., and Schöll E. (2015) *Chaos* **25**, 083104.

Ulonska S., Omelchenko I., Zakharova A., and Schöll E. (2016) *Chaos* **26**, 094825.

Omelchenko I., Maistrenko Y., Hövel P., and Schöll E. (2011) *Phys. Rev. Lett.* **106**, 234102.

Omelchenko I., Riemenschneider B., Hövel P., Maistrenko Y., and Schöll E. (2012) *Phys. Rev. E* **85**, 026212.

Hagerstrom A. M., Murphy T. E., Roy R., Hövel P., Omelchenko I., and Schöll E. (2012) *Nature Phys.* **8**, 658.